Journal of Computational Acoustics, Vol. 23, No. 1 (2015) 1550003 (19 pages)

DOI: 10.1142/S0218396X15500034

INTERNATIONAL ASSOCIATION
FOR MATHEMATICS AND
COMPUTERS IN SIMULATION

A Waveguide-Invariant-Based Warping Operator and Its Application to Passive Source Range Estimation

Yu Bo Qi

State Key Laboratory of Acoustics, Institute of Acoustics
Chinese Academy of Sciences, Beijing 100190, P. R. China

University of Chinese Academy of Sciences
Beijing 100049, P. R. China
qyb@mail.ioa.ac.cn

Shi Hong Zhou*, Ren He Zhang† and Yun Ren‡

State Key Laboratory of Acoustics, Institute of Acoustics
Chinese Academy of Sciences, Beijing, 100190, P. R. China
**shih_zhou@mail.ioa.ac.cn*
†*zrh@mail.ioa.ac.cn*
‡*renyun@mail.ioa.ac.cn*

Received 12 March 2014
Accepted 5 November 2014
Published 31 December 2014

A formula for the instantaneous phase of the cross-correlation function of two different modes using the relationship between the horizontal wavenumber difference and frequency described by the waveguide invariant is deduced in this paper. Based on the formula, a waveguide-invariant-based warping operator suitable for both reflected and refracted modes in shallow water at low frequency is presented, providing an effective tool to filter the cross-correlation function of modes from the signal autocorrelation function. Using the phase of the filtered cross-correlation component in the frequency domain, a passive source ranging method on a single hydrophone is proposed. Simulated and experimental data using impulsive signals verify the validity of the derived warping operator and source ranging method.

Keywords: Waveguide invariant; warping transform; passive source range estimation; autocorrelation function; shallow water.

1. Introduction

In a shallow water waveguide, the low-frequency acoustic field can be viewed as a sum of normal modes. Broadband acoustic propagation has a unique dispersive phenomenon due to the waveguide characteristics of shallow water. The acoustic field is always dominated by a set of normal modes, and the acoustic intensity created by a broadband source exhibits striations when plotted versus range and frequency, because of the interference between different modes. These striations can be characterized by a scalar parameter, called waveguide

invariant.[1,2] As the waveguide invariant summarizes the acoustic dispersion in the waveguide, it is used in various applications, such as source motion compensation,[3] source range estimation,[4] reverberation mitigation,[5] improvement of low-frequency spatial correlation,[6] dedispersion,[7] and time-frequency representations.[8]

A warping transform is a unitary transform, and was first introduced to signal analysis by Baraniuk.[9] If an expression for the signal instantaneous phase is known, the original signal can be transformed to a single frequency signal using a corresponding warping operator through time-axis stretching or compression. Based on the expression for the mode's instantaneous phase for an ideal waveguide with perfect reflection boundaries, Bonnel *et al.* presented the warping operator $h(t) = \sqrt{t^2 + t_r^2}$ to filter normal modes from the signal received by a single hydrophone, where t_r is the arrival time of a signal.[10] This warping operator has been applied to source range estimation,[11,12] geo-acoustic inversion,[13] bubble pulse cancelation[14] and obtaining the difference of the waveguide invariant between modes.[15] Touzé *et al.*[16] and Niu *et al.*[17] build two different warping operators using a Pekeris waveguide model, which have better filtering performance compared with the operator based on an ideal model. Niu *et al.* also present the warping operators for nonisovelocity shallow water waveguides.[18] A frequency waveguide-invariant-based warping operator is also defined by Bonnel *et al.*[8] This operator can transform modes to impulsive signals, making it a useful tool for modal filtering. One should note that all these operators are confined to impulsive sources if the considered signal is the raw received signal (i.e. not the autocorrelation of the received signal). It is required to deconvolve the source influence first for nonimpulsive sources.

Compared to the instantaneous phase of a single mode, the cross-correlation of two modes far from their cut-off frequencies has a similar instantaneous phase expression, i.e. $\phi_{mn}(t) = 2\pi\upsilon_{mn}\sqrt{t^2 - t_r^2}$ in a Pekeris waveguide or iso-speed shallow water environment, where υ_{mn} is the coupled characteristic frequency of modes m and n.[19] So the warping operator $h(t) = \sqrt{t^2 + t_r^2}$ is also applicable to isolate the cross-correlation function of two modes or extract characteristic frequencies of the waveguide from a signal autocorrelation function, which can be used for source range estimation.[19,20] Qi *et al.* deduced modes' characteristic frequencies in a range-dependent waveguide whose bottom bathymetry varies with range using the adiabatic normal mode approximation, and extended this source ranging method to a range-dependent shallow water waveguide.[21]

However, it should be noted that the conventional warping operator $h(t)$ is valid for a signal consisting of reflection dominated modes in shallow water. In other words, it is suitable for the shallow water waveguides with a waveguide invariant approximately equal to one. It implies that the horizontal wavenumber difference between two modes is inversely proportional to the frequency. But in a waveguide with a thermocline or a surface channel, the waveguide invariant varies over a range of values, especially for the refraction dominated modes. The instantaneous phase of the cross-correlation function of modes m and n no longer satisfies $\phi_{mn}(t) = 2\pi\upsilon_{mn}\sqrt{t^2 - t_r^2}$, thus the performance of the warping operator $h(t) = \sqrt{t^2 + t_r^2}$ will be significantly degraded. So a novel warping operator is necessary for these waveguides. An expression of the instantaneous phase of the cross-correlation function,

which can be deduced through an inverse Fourier transform of the phase expression in the frequency domain, is the precondition for proposing an appropriate warping operator. Although it is impossible to get an accurate analytic phase solution for these complex environments, using the wavenumber difference described by the waveguide invariant, we can obtain an approximate expression.

The remainder of this paper is organized as follows. In Sec. 2, a formula is derived for the instantaneous phase of the cross-correlation function of two modes, based on the horizontal wavenumber difference described by the waveguide invariant. The corresponding waveguide-invariant-based warping operator and its connection with the traditional operator are presented. Section 3 describes one source ranging method using the phase of the filtered cross-correlation function in the frequency domain. Section 4 presents the results using simulated and experimental data. Finally, the conclusion is provided in Sec. 5.

2. Warping Operator Based on Waveguide Invariant

2.1. *β-warping operator*

Low-frequency acoustic propagation can be described by normal mode theory in shallow water. Considering a broadband source emitting a signal in a range-independent waveguide, the received pressure field is given by[22]

$$P(f) = S(f) \sum_{m=1}^{M} A_m(f) e^{jk_{rm}(f)r}, \tag{1}$$

where $S(f)$ is source spectrum, $k_{rm}(f)$ represents the modal horizontal wavenumber with index m at frequency f, r is the range, M denotes the number of propagating modes, and $A_m(f)$ is the amplitude. $A_m(f) = \frac{1}{\rho\sqrt{8\pi r}}\psi_m(z_s)\psi_m(z)\frac{e^{j\pi/4}}{\sqrt{k_{rm}f}}$, where $\psi_m(z)$ represents the modal function of index m, z_s and z are the source and receiver depth, respectively, and ρ represents the water density at the source depth. The horizontal wavenumber is a function of the index m and f as the modal propagation is dispersive.

The autocorrelation function of the received signal in the time domain is obtained as the inverse Fourier transform of the power spectral density,

$$R(r,t) = \int_{-\infty}^{\infty} |S(f)|^2 \left(\sum_{m=1}^{M} |A_m(f)|^2 e^{j2\pi ft} + \sum_{n=1}^{M} \sum_{m\neq n}^{M} A_n(f) A_m^*(f) e^{j(k_{rn}(f)-k_{rm}(f))r + j2\pi ft} \right) df, \tag{2}$$

where * denotes the complex conjugation operator. The first integral term is the sum of all modes' autocorrelation function, while the second integral term represents the cross-correlation function of different modes. If M propagating modes exist, there are $\frac{M!}{(M-2)!2!}$ combinations of two different modes.

In an actual shallow water waveguide, it is impossible to get an accurate analytic expression for the wavenumber difference as a function of sound speed, bottom parameters, and frequency. However, the mode wavenumber difference and the frequency satisfy the following power law relationship,[23,24]

$$\Delta k_{mn}(f) = k_{rn}(f) - k_{rm}(f) = -\gamma_{nm} f^{-\frac{1}{\beta}}, \tag{3}$$

where γ_{nm} is a constant which depends on the mode number (γ_{nm} can be calculated by curve fitting when wavenumber differences at different frequencies are available), and β is the waveguide invariant. One should note that the waveguide invariant is only invariant within a mode group and frequency interval,[22] Rouseff *et al.* define the local invariant in terms of the phase velocity ν_m and the group velocity μ_m as[25]

$$\beta_{mn} = -\frac{\dfrac{1}{\nu_m} - \dfrac{1}{\nu_n}}{\dfrac{1}{\mu_m} - \dfrac{1}{\mu_n}}. \tag{4}$$

For one pair of modes with $\beta_{mn} > 0$, the lower mode has a higher group velocity and arrives at the receiver first, while the higher mode propagates faster in the case of $\beta_{mn} < 0$. Only considering the right-side of the waveform of the symmetrical autocorrelation function $R(r,t)$ from the peak and ignoring the mode's autocorrelation component, the sum of the cross-correlation functions of two different modes is given by

$$R_2(r,t) = \begin{cases} \displaystyle\sum_{n=1}^{M}\sum_{m>n}^{M}\int_{-\infty}^{\infty} |S(f)|^2 A_m^*(f) A_n(f) e^{j\Delta k_{mn}(f) r + j2\pi f t} df & \text{if } \beta_{mn} > 0 \\ \displaystyle\sum_{n=1}^{M}\sum_{m>n}^{M}\int_{-\infty}^{\infty} |S(f)|^2 A_m(f) A_n^*(f) e^{-j\Delta k_{mn}(f) r + j2\pi f t} df & \text{if } \beta_{mn} < 0 \end{cases}. \tag{5}$$

Now, we focus on the case of $\beta_{mn} > 0$. Let

$$\varphi_{mn}(r,f) = \Delta k_{mn}(f) r \tag{6}$$

and

$$B_{mn}(f) = |S(f)|^2 A_m^*(f) A_n(f). \tag{7}$$

It is convenient to recast Eq. (5) in the following abbreviated form,

$$R_2(r,t) = \sum_{n=1}^{M}\sum_{m>n}^{M}\int_{-\infty}^{\infty} B_{mn}(f) e^{j(\varphi_{mn}(r,f) + 2\pi f t)} df. \tag{8}$$

For flat spectrum sources with $|S(f)|$ slowly changing with f, the amplitude of the integral term is considered to be a slowly varying function of frequency compared to the phase

dependence. Applying the method of stationary phase[26] to approximate this integral yields

$$R_2(r,t) \approx \sum_{n=1}^{M}\sum_{m>n}^{M} B_{mn}(f_{mns})\sqrt{\frac{2\pi}{\varphi''_{mn}(r,f_{mns})}}e^{j\frac{\pi}{4}sgn(\varphi''_{mn}(r,f_{mns}))}e^{j(\varphi_{mn}(r,f_{mns})+2\pi f_{mns}t)}, \quad (9)$$

where $''$ denotes second derivative in frequency, sgn is the signum function, and f_{mns} are the stationary phase points obtained by solving

$$\frac{\partial\varphi_{mn}(r,f)}{\partial f} + 2\pi t = 0. \quad (10)$$

Acorrding to Eqs. (6) and (3), one can rewrite Eq. (10) as

$$2\pi t + \frac{1}{\beta_{mn}}\gamma_{nm} f^{-\frac{1}{\beta_{mn}}-1} r = 0. \quad (11)$$

By solving the above equation, the stationary phase points can be expressed as

$$f_{mns}(t) = \left(-\frac{r}{2\pi\beta_{mn}}\gamma_{nm}\right)^{\frac{\beta_{mn}}{1+\beta_{mn}}} t^{-\frac{\beta_{mn}}{1+\beta_{mn}}}. \quad (12)$$

Inserting Eq. (12) into Eq. (9) and ignoring $e^{j\frac{\pi}{4}sgn(\varphi''_{mn}(r,f_{mns}))}$, the instantaneous phase of the cross-correlation function of modes m and n can be expressed as

$$\begin{aligned}\phi_{mn}(t) &= \varphi_{mn}(r,f_{mns}(t)) + 2\pi f_{mns}(t)t = -r\gamma_{nm}(f_{mns}(t))^{-\frac{1}{\beta_{mn}}} + 2\pi f_{mns}(t)t \\ &= 2\pi\left(-\frac{r}{2\pi\beta_{mn}}\gamma_{nm}\right)^{\frac{\beta_{mn}}{1+\beta_{mn}}}(1+\beta_{mn})t^{\frac{1}{1+\beta_{mn}}}. \end{aligned} \quad (13)$$

We therefore define a waveguide-invariant-based warping operator (β-warping operator) according to Eq. (13),

$$\tilde{h}(t) = t^{1+\beta_{mn}}, \quad (14)$$

and its corresponding inverse warping operator is given by

$$\tilde{h}^{-1}(t) = t^{\frac{1}{1+\beta_{mn}}}. \quad (15)$$

Warping the time coordinate and re-sampling such that $\tilde{t} = t^{1+\beta_{mn}}$ transforms the modal cross-correlation functions into a series of monotones at frequencies

$$\varsigma_{mn}(r) = \left(-\frac{r}{2\pi\beta_{mn}}\gamma_{nm}\right)^{\frac{\beta_{mn}}{1+\beta_{mn}}}(1+\beta_{mn}). \quad (16)$$

Following an identical derivation, we can obtain the corresponding frequency of the warped cross-correlation function for the case of $\beta_{mn} < 0$ as shown below:

$$\varsigma_{mn}(r) = \left(-\frac{r}{2\pi\beta_{mn}}\gamma_{mn}\right)^{\frac{\beta_{mn}}{1+\beta_{mn}}}(1+\beta_{mn}) = \left(\frac{r}{2\pi\beta_{mn}}\gamma_{nm}\right)^{\frac{\beta_{mn}}{1+\beta_{mn}}}(1+\beta_{mn}). \quad (17)$$

In a real shallow water waveguide, there may exist both reflection dominated modes and refraction dominated modes. Although the values of the waveguide invariant are different for different pairs of modes, the received signal at a given range is usually dominated by a group of modes that lie within a small range of β values. This group of modes determines the value of the waveguide invariant we choose to apply with the β-warping transform.

2.2. *Connection between β-warping operator and the traditional warping operator*

Now we consider the internal connection between the β-warping operator $\tilde{h}(t) = t^{1+\beta}$ and the traditional operator $h(t) = \sqrt{t^2 + t_r^2}$. When the waveguide invariant equals unity, according to Eq. (13), the instantaneous phase of the cross-correlation function can be expressed as

$$\phi_{mn}(t) = 2\pi\sqrt{-\frac{c}{\pi}\gamma_{nm}}\sqrt{2t_r}\sqrt{t}, \tag{18}$$

where $t_r = r/c$, and c equals the average sound speed in water for nonisovelocity waveguides. The autocorrelation function of the received signal is time shifted by t_r to bring the peak of the function to be time t_r before being transformed by the traditional warping operator,[19] and then the instantaneous phase becomes

$$\phi_{mn}(t - t_r) = 2\pi\sqrt{-\frac{c}{\pi}\gamma_{nm}}\sqrt{2t_r}\sqrt{t - t_r}. \tag{19}$$

For lower modes far from cut-off frequencies, the amplitude of their cross-correlation function decreases rapidly to zero as t increases. The time spread $\triangle t$ of their cross-correlation function is much smaller compared with t_r, so when $t_r \leq t < t_r + \triangle t$, $\phi_{mn}(t - t_r)$ can be approximated by

$$\phi_{mn}(t - t_r) \approx 2\pi\sqrt{-\frac{c}{\pi}\gamma_{nm}}\sqrt{t + t_r}\sqrt{t - t_r} = 2\pi\sqrt{-\frac{c}{\pi}\gamma_{nm}}\sqrt{t^2 - t_r^2}. \tag{20}$$

Warping the time coordinate and re-sampling such that $\tilde{t} = \sqrt{t^2 + t_r^2}$, the warped modal cross-correlation function can be expressed as

$$W_h\phi_{mn}(t - t_r) = 2\pi\sqrt{-\frac{c}{\pi}\gamma_{nm}t}. \tag{21}$$

So the traditional warping operator can transform the cross-correlation function to a signal with a single frequency

$$\upsilon_{mn} = \sqrt{-\frac{c}{\pi}\gamma_{nm}}. \tag{22}$$

From the above analysis, we can conclude that both the β-warping operator $\tilde{h}(t) = t^{1+\beta}$ and the traditional operator $h(t) = \sqrt{t^2 + t_r^2}$ can transform the cross-correlation function to a monotone frequency when the waveguide invariant approximately equals unity. One

should note that the cross-correlation function should be time shifted by t_r before being transformed by the traditional warping operator. Otherwise, only the β-warping operator is suitable. Comparing the traditional warping operator and the β-warping operator, we can also find that the former uses the source range as a parameter (while it is unnecessary to know the real source range, in a practical scenario one can assume a range to apply the transformation when the real source range is unknown[19]) and the frequency of the warped cross-correlation function is invariant, independent of source range. This characteristic is used for source range estimation by Zhou *et al.*[19,20] Since the β-warping operator proposed in this paper does not need the source range, the cross-correlation function filtering can be performed without knowledge of source position. Application of the filtered cross-correlation in source ranging will be discussed in the next section.

3. Source Range Estimation

From the previous analysis, we can see that the warping transform provides an effective method to separate the cross-correlation function of modes from the signal autocorrelation function. It is worth mentioning that as long as the source spectrum is relatively flat to make the stationary phase approximation in Eq. (9) tenable, the β-warping operator can be used as the core of a filtering scheme to isolate the cross-correlation component by following the steps below:

(1) Obtain the autocorrelation function $R(r,t)$ of the received signal.
(2) Only consider the right-side waveform of the symmetrical autocorrelation function $R(r,t)$ from the peak and delete the mode's autocorrelation component (the mode's autocorrelation component is concentrated near the peak compared with the cross-correlation component, so zeroing the signal autocorrelation near the peak can delete it to a large extent) to get the sum of different combinations of modal cross-correlation functions, i.e. $R_2(r,t)$.
(3) Warp $R_2(r,t)$ using the β-warping operator $\tilde{h}(t) = t^{1+\beta}$ to obtain $W_{\tilde{h}}R_2(r,t)$.
(4) Isolate the warped cross-correlation function $W_{\tilde{h}}R_{mn}(r,t)$ of modes m and n from $W_{\tilde{h}}R_2(r,t)$ by using a narrow band filter.
(5) Unwarp $W_{\tilde{h}}R_{mn}(r,t)$ using the inverse warping operator $\tilde{h}^{-1}(t) = t^{\frac{1}{1+\beta}}$ to get the filtered cross-correlation $R_{mn}(r,t)$ in the original time domain.

The above steps are similar to the method in Bonnel's paper,[13] where the traditional warping operator is used to filter modes from the received signal. Because the phase of the cross-correlation function in the frequency domain contains source range information (see Eq. (6)), the isolated modal cross-correlation function can be used for source ranging. There are two challenges for obtaining range information from the measured phase of the modal cross-correlation function. One is the sign difference of modal eigenfunctions at the source and receiver depths, i.e. the sign of $\psi_m(z_s)\psi_m(z)\psi_n(z_s)\psi_n(z)$, which can be circumvented by squaring (not the absolute squaring) the filtered cross correlation function. The other challenge is the ambiguity on the measured phase, since the phase is measured on the Fourier

domain and is only known modulo 2π. In this paper, this challenge can be solved in the broadband configuration. The measured phase of the squared cross-correlation function of modes m and n at frequency f and reference frequency f_0 can be written as

$$\vartheta_{mn}(r, f) = 2\Delta k_{mn}(f)r - 2l\pi, \tag{23a}$$

$$\vartheta_{mn}(r, f_0) = 2\Delta k_{mn}(f_0)r - 2l\pi, \tag{23b}$$

respectively, where l is an integer, so the difference of the measured phase at f and f_0 is

$$\Delta\vartheta_{mn}(r, f) = 2(\Delta k_{mn}(f) - \Delta k_{mn}(f_0))r. \tag{24}$$

From Eq. (24), we can see that the measured phases at different frequencies of the squared cross-correlation component changes linearly with wavenumber differences, so source range estimation with a single receiver can be performed by linear regression of the measured phases and wavenumber differences computed by the normal mode model.

Now we compare the difference of the warping transform of signal itself and the signal autocorrelation function. When the object to be transformed is the signal itself, the warping operator is confined to impulsive sources, so Bonnel *et al.* deconvolve the source influence first when using the warping transform to range bowhead whale sounds from a single receiver.[12] When the object to be transformed is the signal autocorrelation function, the warping operator does not have this restriction as the phase of the source is deleted automatically due to the autocorrelation processing (see Eq. (2)).

4. Application in Simulated and Experimental Data

4.1. *Simulated data*

In order to verify the above theoretical analysis, simulated signals in an ideal waveguide and a n^2-linear refracting waveguide computed with KRAKEN[27] will be processed in this subsection.

4.1.1. *Ideal waveguide*

The ideal waveguide is first analyzed with the following simulation parameters: sound speed 1500 m/s, water depth 100 m, source depth 100 m, and receiver depth 100 m. The frequency of the emitted signal is from 100 Hz to 200 Hz. Figure 1(a) shows the spectrum of the warped cross-correlation function of modes 2 and 1 at different ranges using the traditional warping operator. The characteristic frequency υ_{21} is independent of source range. For comparison, Fig. 1(b) shows the result of using the β-warping operator, where the dashed line represents theoretical frequencies $\varsigma_{21}(r)$ calculated by Eq. (16). Here, $\beta = 1$, $m = 2$ and $n = 1$ for $\gamma_{12} = -\pi\frac{f_{c2}^2 - f_{c1}^2}{c}$(In the ideal waveguide, $k_{rm}(f) - k_{rn}(f) \approx \frac{2\pi}{c}(f - \frac{f_{cm}^2}{2f}) - \frac{2\pi}{c}(f - \frac{f_{cn}^2}{2f}) = -\pi\frac{f_{cm}^2 - f_{cn}^2}{c}f^{-1}$, where f_{cm} denotes the cut-off frequency of mode m. Comparing with Eq. (3), $\gamma_{12} = -\pi\frac{f_{c2}^2 - f_{c1}^2}{c}$).[19] For lower modes far from cut-off in an ideal waveguide, the waveguide

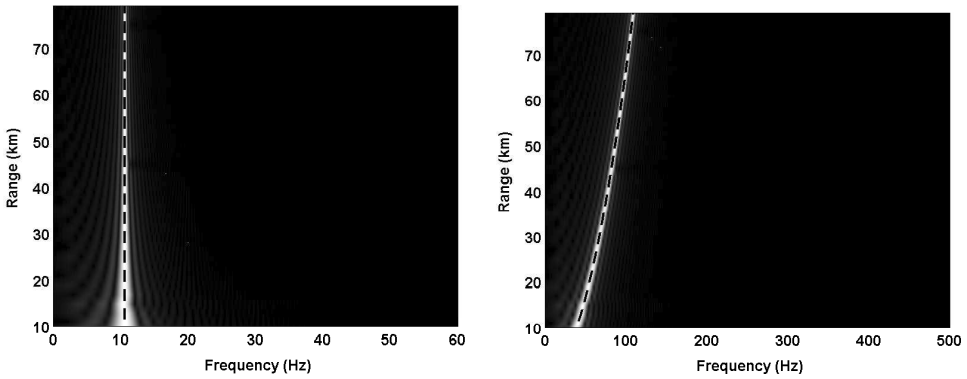

(a) (b)

Fig. 1. Spectrum of warped cross-correlation function of modes 2 and 1 at different ranges using traditional warping and β-warping operators in the case of an ideal waveguide. (a) Traditional operator (dashed line represents theoretical frequencies calculated by Eq. (22)); (b) β-warping operator using $\beta = 1$ (dashed line represents theoretical frequencies calculated by Eq. (16) with $\gamma_{12} = -\pi \frac{f_{c2}^2 - f_{c1}^2}{c}$).

invariant approximately equals unity, so both the traditional operator and the β-warping operator can transform their cross-correlation function into a narrow band or line spectrum.

4.1.2. *n^2-linear refracting waveguide*

Now we discuss the results of the signal autocorrelation function in an n^2-linear refracting waveguide. The water sound speed at the surface and bottom are 1500 m/s and 1560 m/s, respectively. The water depth is 100 m and the bottom parameters of sound speed, density, and attenuation are given by $c_b = 1600$ m/s, $\rho_b = 1.8\,\mathrm{g/cm^3}$ and $\alpha_b = 0.1\,\mathrm{dB}/\lambda$, respectively. Both source and receiver are set at 15 m. The frequency of the emitted signal is from 100 Hz to 200 Hz. In this scenario, all propagating modes are considered. The acoustic intensity versus range and frequency is presented in Fig. 2(a). The first three refracted modes dominate the received sound field while the higher reflected modes are weakly excited and attenuate quickly, resulting in the striations with a negative slope in Fig. 2(a). The waveguide invariant computed by Eq. (4) for different pairs of modes is illustrated in Fig. 2(b). The value of the waveguide invariant for these three pairs is almost the same, approximately equal to -3 for frequencies far away from the modal cut-off. While in the low frequency band (from 100 Hz to 120 Hz), the value has a significant change except for the pair of modes 1 and 2.

Figure 3 presents the spectrum of the warped signal autocorrelation at different ranges using traditional and β-warping operators($\beta = -3$). From Fig. 3(a), we can see that it is impossible to distinguish different pairs of cross-correlation components in the spectrum, so the traditional warping operator is not suitable to isolate different pairs of modes from the signal autocorrelation function. As for the β-warping operator, there are two obvious curves, representing the cross-correlation of modes 1 and 2 and modes 1 and 3, respectively, in Fig. 3(b), where the absolute values of theoretical frequencies of modes 1 and 2 and modes 1 and 3 calculated by Eq. (17) are also presented as dashed lines (here, $m = 2$ and

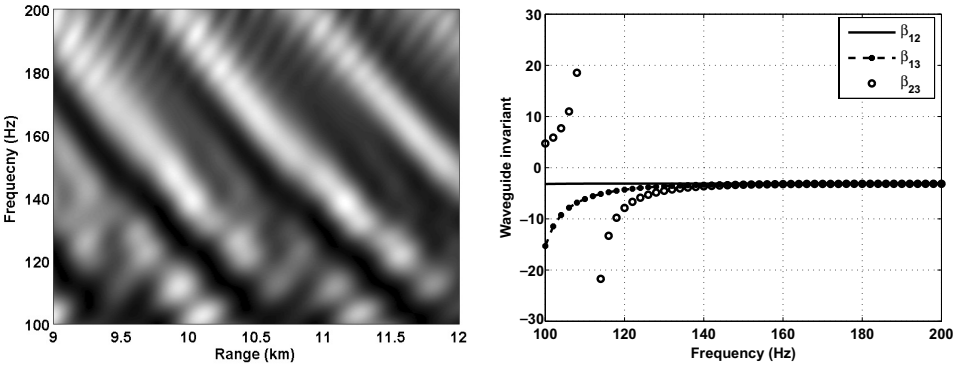

(a) (b)

Fig. 2. Acoustic intensity and waveguide invariant for the n^2-linear refracting waveguide. (a) Acoustic intensity versus range and frequency; (b) Waveguide invariant value computed by Eq. (4) for different pairs of modes.

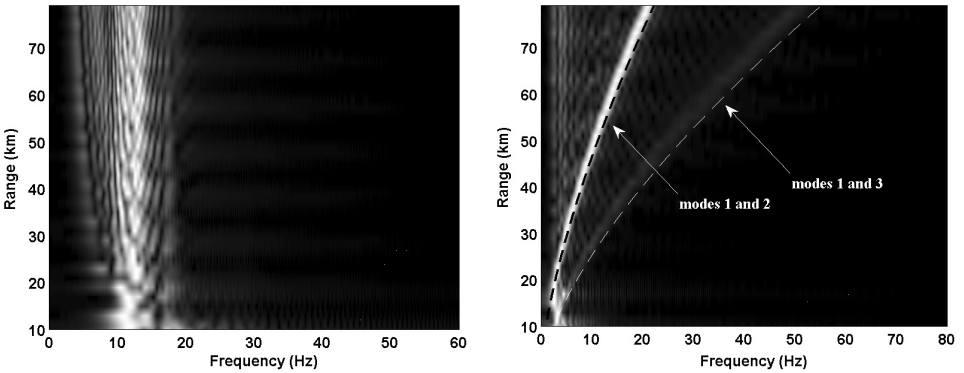

(a) (b)

Fig. 3. Spectrum of warped signal autocorrelation at different ranges using traditional warping and β-warping operators in the case of n^2-linear refracting waveguide. (a) Traditional operator; (b) β-warping operator using $\beta = -3$ (dashed lines represent theoretical frequencies of modes 1 and 2, and modes 1 and 3 at different ranges calculated by Eq. (17) respectively with $\gamma_{12} = -1.19 \times 10^{-3}$, $\gamma_{13} = -2.18 \times 10^{-3}$).

$n = 1$ for $\gamma_{12} = -1.19 \times 10^{-3}$, and $m = 3$ and $n = 1$ for $\gamma_{13} = -2.18 \times 10^{-3}$, calculated by curve fitting of wavenumber differences and Eq. (3)). It is easy to isolate these two pairs of cross-correlation components from the signal autocorrelation using narrow-band filtering. As the energy of the cross-correlation function of modes 2 and 3 are much smaller compared with two other pairs, we can not see its corresponding curve in Fig. 3(b).

The spectrum of the warped autocorrelation function for a signal emitted at 35 km range is presented in Fig. 4 as a black line. There are two main peaks corresponding to the cross-correlation of modes 1 and 2, and modes 1 and 3. Incomplete deletion of the modes' autocorrelation function contributes to the raised spectrum before the biggest peak. The cross-correlation filtering result is given in Fig. 5, where the 3 traces correspond to,

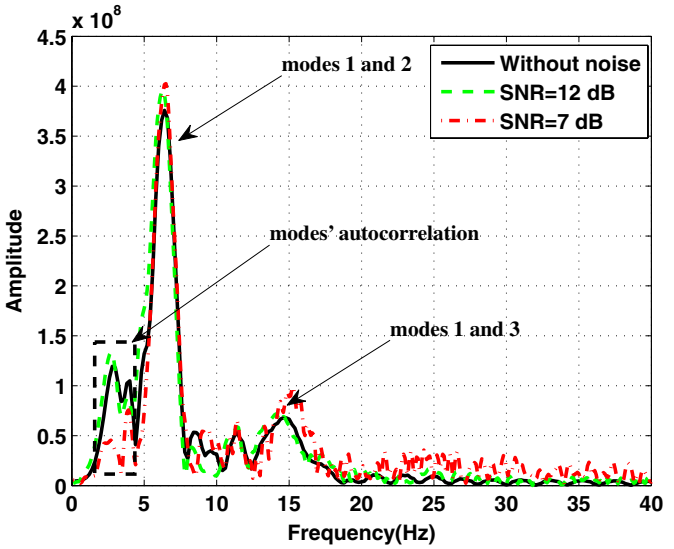

Fig. 4. (Color online) Spectrums of the warped autocorrelation function for signal emitted at 35 km in different background noisy environments using β-warping operator ($\beta = -3$) in the case of n^2-linear refracting waveguide. The signal autocorrelation before 0.04 s is set to zero to delete the modes' autocorrelation component.

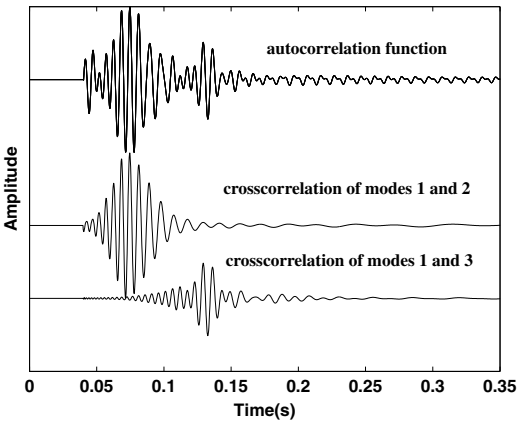

Fig. 5. Cross-correlation filtering result in the case of n^2-linear refracting waveguide. Three traces correspond to, from top to bottom, signal autocorrelation, filtered cross-correlation of modes 1 and 2, filtered cross-correlation of modes 1 and 3, respectively.

from top to bottom, signal autocorrelation, filtered cross-correlation of modes 1 and 2, and filtered cross-correlation of modes 1 and 3, respectively. Source ranging results using the phase of the filtered cross-correlation function in the frequency domain are illustrated in Fig. 6. The linear regression result of modes 1 and 2 is 34.95 km with 0.03 km uncertainty at the 95% confidence level. There are two reasons which contribute to the error. One is the incomplete deletion of the modes' autocorrelation component. The other reason is the

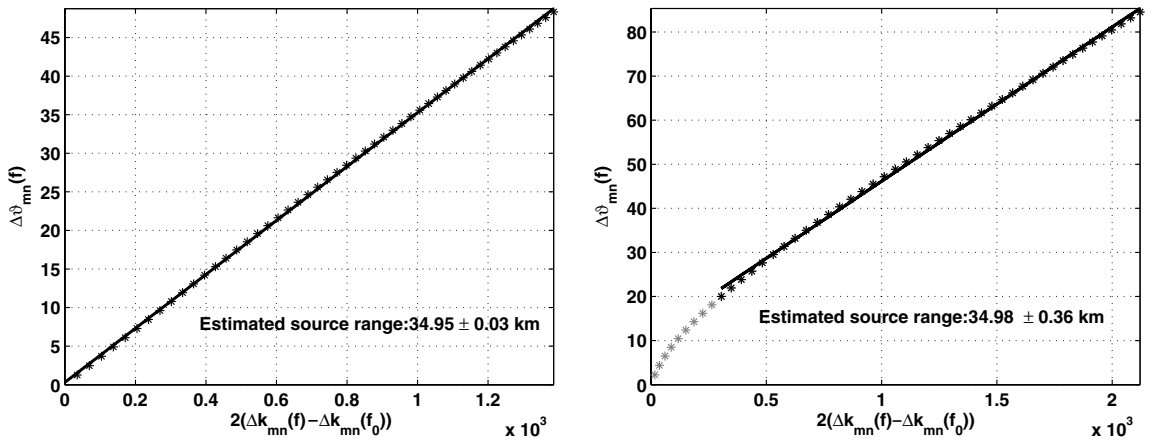

(a) (b)

Fig. 6. Source ranging results by linear regression between the measured phases of the filtered cross-correlation function and wavenumber differences computed by the normal mode model. (a) Modes 1 and 2; (b) Modes 1 and 3.

imperfect performance of the square window filter to isolate the cross-correlation component. The ranging result is acceptable in spite of the small error.

As for the pair of modes 1 and 3, we can see that the phase of the filtered cross-correlation function does not change linearly with wavenumber difference in the frequency band from 100 Hz to 120 Hz (gray points in Fig. 6(b)). The significant variation of the waveguide invariant for modes 1 and 3 results in the performance of the β-warping operator being nonlinear. However, the phase of the filtered cross-correlation function changes linearly with wavenumber difference in frequency band from 120 Hz to 200 Hz, and the source ranging result using this frequency band is still acceptable. From the discussion above, we conclude that β-warping operator works well in the frequency band where there is no large variation of the value of the waveguide invariant, such as for frequencies far away from modal cut-off.

To demonstrate that the filtering procedure and source ranging method can be effective in an experimental context, the β-warping operator is applied to synthetic data in the presence of white Gaussian noise. The spectrums of the warped autocorrelation function in different background noisy environments are given in Fig. 4. In this paper, the Signal-to-Noise Ratio (SNR) is computed over the time window of the impulsive signal with the same frequency band. When SNR equals 7 dB, there are still two obvious peaks in the spectrum. The source ranging result of modes 1 and 2 is 34.84 km with 0.18 km uncertainty at the 95% confidence level, while it is 35.23 km with 0.31 km uncertainty for modes 1 and 3.

In a real experimental configuration, it is hard to get an accurate waveguide invariant value. So the performance of the β-warping operator with a small waveguide invariant error is discussed below. Figure 7 illustrates the spectrum of the warped autocorrelation function for a signal emitted at 35 km using the β-warping operator with $\beta = -4$. Although the choice of the waveguide invariant value affects the corresponding frequency of cross-correlation

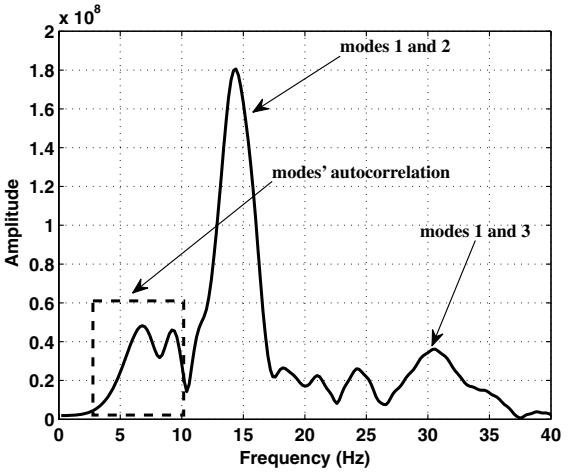

Fig. 7. Spectrum of the warped autocorrelation function for a signal emitted at 35 km using β-warping operator ($\beta = -4$) in the case of an n^2-linear refracting waveguide.

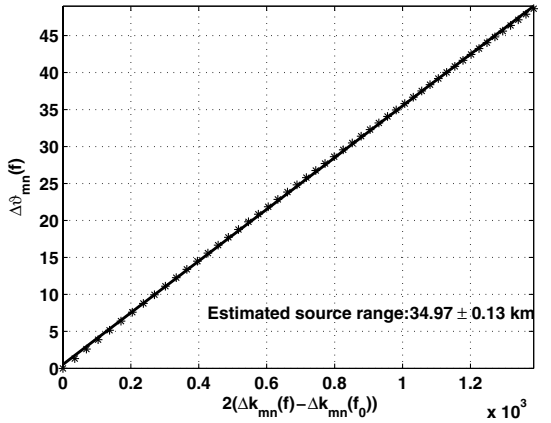

Fig. 8. Source ranging result by linear regression between the measured phases of the filtered cross-correlation function of modes 1 and 2 using the β-warping operator ($\beta = -4$) and wavenumber differences computed by a normal mode model.

function of modes, the characteristics of the warped spectrum remain unchanged, still containing two obvious peaks. The source ranging result using the filtered cross-correlation function of modes 1 and 2 is also shown in Fig. 8. The above simulation results verify the robustness of β-warping operator.

4.2. *Experimental data*

This subsection presents the results for one signal received in the sound propagation measurement experiment in the north Yellow Sea on December 19 to 20, 2011. Explosive charges [38-g charges of trinitrotoluene (TNT)] were used as the sources. The source depth was 25 m below the sea surface. The bathymetry was almost flat between the source and receiver, the

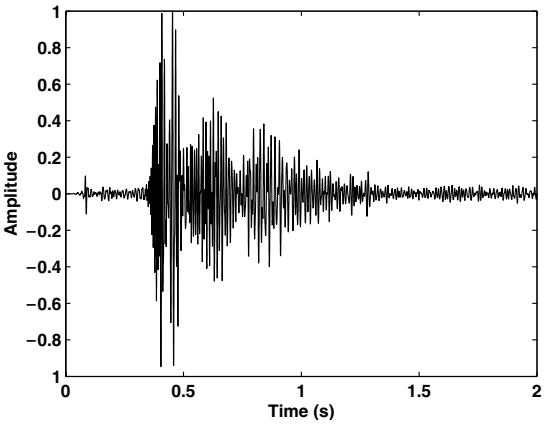

Fig. 9. Normalized waveform of the signal emitted at 25.2 km range.

mean water depth was 73 m with about 3 m variability. Sound speed in the water was almost constant, with a value of 1480 m/s. The received signals were recorded by a 32-element, 300 m-length horizontal array.

Figure 9 shows the normalized waveform of the signal recorded by the first hydrophone after band-pass filtering from 60 Hz to 200 Hz. The source range recorded by the Global Position System (GPS) was 25.2 km. After zeroing different lengths of the signal's autocorrelation function to delete the modes' autocorrelation component, the spectrums of the warped signal's autocorrelation function using the β-warping operator ($\beta = 1$) are illustrated in Fig. 10, where τ represents the length of the zeroed signal's autocorrelation function. As shown in the figure, there are three main peaks from 50 Hz to 200 Hz for these three spectrums, corresponding to the cross-correlation of modes 1 and 2, modes 2 and 3, and modes 1 and 3. The spectrum of $\tau = 0.3$ has the clearest structure due to little remaining of the modes' autocorrelation component, while incomplete deletion of the

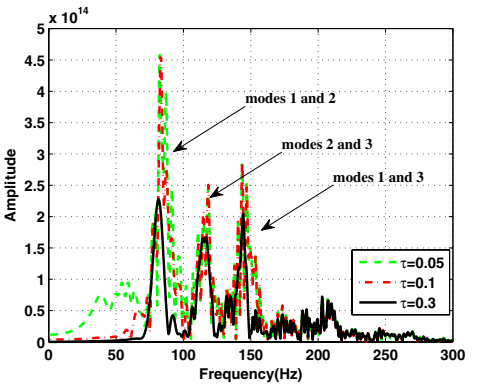

Fig. 10. (Color online) Spectrums of the warped autocorrelation function of the experimental signal emitted at 25.2 km range. τ represents the length of the zeroed signal's autocorrelation function.

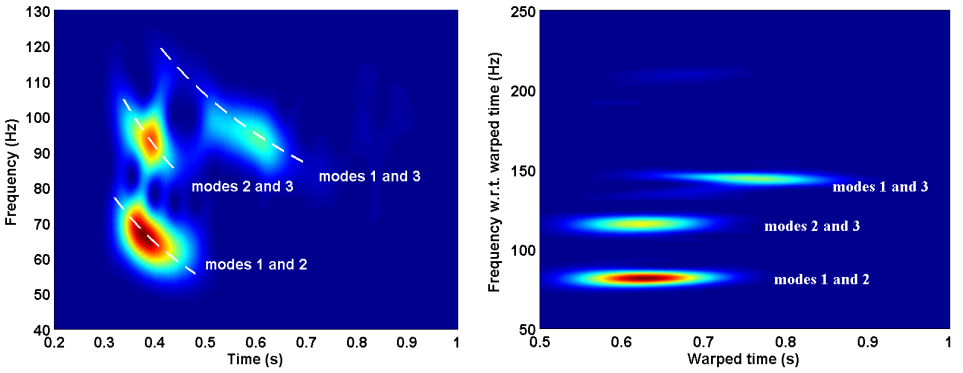

(a) (b)

Fig. 11. (Color online) Spectrograms of the signal autocorrelation function and the warped signal autocorrelation function. (a) Signal autocorrelation function; (b) Warped signal autocorrelation function.

modes' autocorrelation component causes the fluctuation in the two other spectrums. So $\tau = 0.3$ is considered in the subsequent analysis.

The spectrogram of the autocorrelation function of the signal is presented in Fig. 11(a). As shown in the figure, the cross-correlation of two modes has the similar dispersion characteristics as the mode itself. In comparison, Fig. 11(b) illustrates the spectrogram of the warped autocorrelation function. It shows that the modal cross-correlation components are approximately transformed to monotone frequencies and they have become perfectly separated from each other. The cross-correlation filtering result is given in Fig. 12, where the 4 traces are, from top to bottom, the signal's autocorrelation, filtered cross-correlation of modes 1 and 2, filtered cross-correlation of modes 2 and 3, and filtered cross-correlation of modes 1 and 3, respectively.

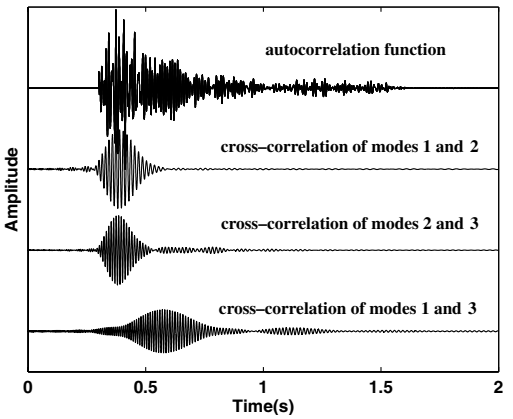

Fig. 12. Cross-correlation filtering result of the experimental signal emitted at 25.2 km range. Four traces correspond to, from top to bottom, signal autocorrelation, filtered cross-correlation of modes 1 and 2, filtered cross-correlation of modes 2 and 3, and filtered cross-correlation of modes 1 and 3, respectively. The signal autocorrelation before 0.3 s is set to zero to delete the modes' autocorrelation component.

Table 1. Sediment parameters and source ranging results by linear regression.

Sediment Type	Sound Speed (m/s)	Density (g/cm^3)	Attenuation (dB/m/kHz)	Estimated range		
				Modes 1 and 2 (km)	Modes 2 and 3 (km)	Modes 1 and 3 (km)
Silt clay	1580	1.58	0.11	26.26 ± 0.13	24.93 ± 0.26	24.65 ± 0.21
Silt sand	1670	1.81	0.69	24.56 ± 0.09	22.32 ± 0.13	22.41 ± 0.11
Fine sand	1750	1.95	0.51	24.01 ± 0.08	21.71 ± 0.11	21.83 ± 0.10

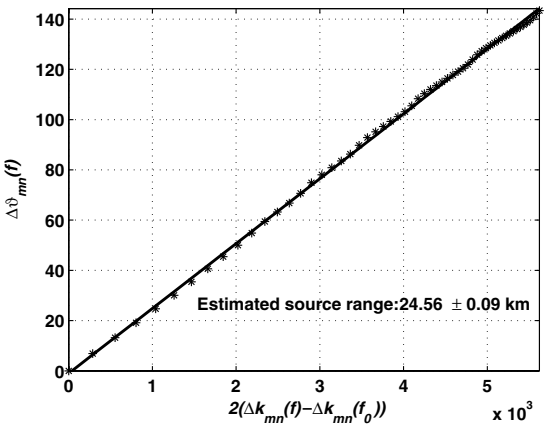

Fig. 13. Source ranging result of the experimental signal by linear regression between the measured phases of the filtered cross-correlation function of modes 1 and 2 and wavenumber differences for the silt sand sediment computed by a normal mode model.

As we do not have detailed information about the sea bottom, three different sediments (silt clay, silt sand and fine sand) are considered in this paper. Sediment parameters and estimated source ranges using different modal combinations are given in Table 1. Besides, Fig. 13 illustrates the linear regression result of the filtered cross-correlation function of modes 1 and 2 for the silt sand sediment. As shown in Table 1, for the same sediment, each modal combination has different estimated ranges. But this difference is acceptable compared with the source range. The estimated ranges of silt clay are the largest as their modal horizontal wavenumber differences are the smallest compared with other sediments (see Fig. 14). The mean estimated ranges of silt clay, silt sand and fine sand are 25.28 km, 23.10 km and 22.52 km, respectively. Source ranging results of all the signals received in the experiment using the modal horizontal wavenumber of the silt clay are illustrated in Fig. 15. All the autocorrelation functions before 0.3 s are set to zero to delete the modes' autocorrelation components. The relative error between the estimated range and the actual value is basically less than 12%, as shown in Fig. 15(b). The mean relative error is about 4%. The above results verify that the β-warping operator performs adequately in this experimental scenario.

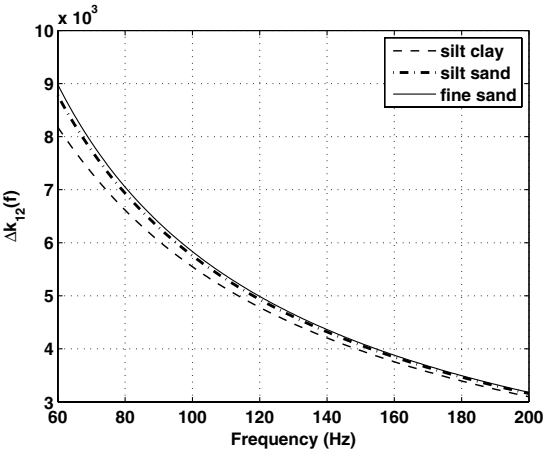

Fig. 14. Horizontal wavenumber difference of modes 1 and 2.

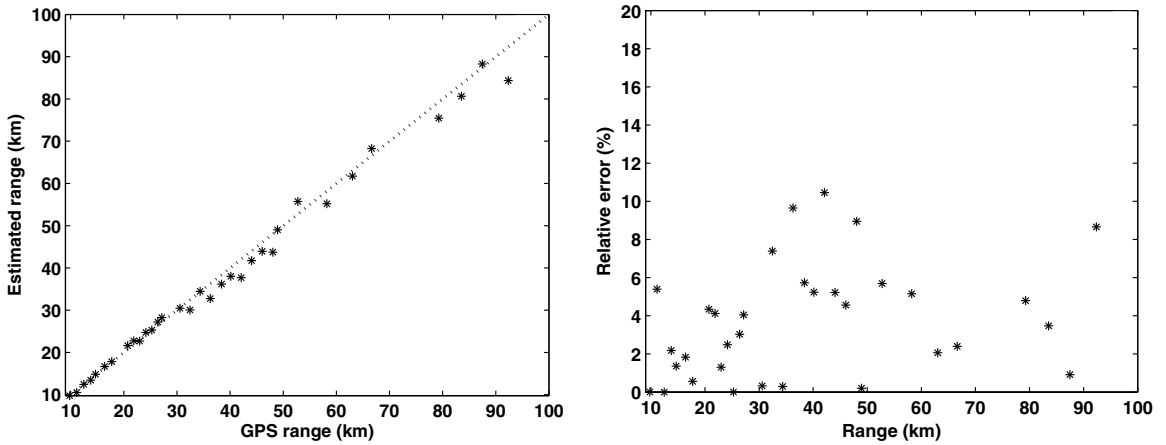

(a) (b)

Fig. 15. Source ranging results of all the signals received in the experiment. (a) Comparison of the estimated range and the GPS range; (b) Relative error between the estimated range and the actual value.

5. Summary

The warping transform provides an effective method to isolate the cross-correlation function of modes or extract the characteristic frequencies of the waveguide from the signal autocorrelation function in shallow water at low frequency. The traditional warping operator is confined to a shallow water environment with the waveguide invariant approximately equal to unity. This paper presents a waveguide-invariant-based warping operator with a wider range of applications. To obtain the warping operator, the instantaneous phase expression of the cross-correlation function of two normal modes is also derived based on the wavenumber difference described by the waveguide invariant. The phase of the filtered

cross-correlation in the frequency domain contains source range information, so using the phase information and wavenumber difference calculated by KRAKEN, single hydrophone passive source ranging is realized on the simulated data of an n^2-linear refracting waveguide and with experimental data. As this paper mainly focuses on the physical meaning of the β-warping operator and its potential use for source ranging, only the impulsive source is considered. Further research and more endeavors are needed in the future engineering applications.

Acknowledgments

This research was supported in part by the National Natural Science Foundation of China under Grant Nos. 11174312 and 11125420, and in part by the Hundred Talents Program of the Chinese Academy of Sciences and China Scholarship Council. The authors would like to thank the two anonymous reviewers for their constructive comments and suggestions to improve the quality of the paper. They are also grateful to Dr. Eric Thorsos in the Applied Physics Laboratory of the University of Washington for polishing the paper.

References

1. S. D. Chuprov, Interference structure of a sound field in a layered ocean, in *Acoustics of Ocean: Current Status*, eds. L. M. Brekhovskikh and I. B. Andreevoi (Nauka, Moscow, 1982), pp. 71–91.
2. L. M. Brekhovskikh and Y. P. Lysanov, *Fundamentals of Oceanic Acoustics*, 2nd edn. (Springer-Verlag, New York, 1991), pp. 140–145.
3. L. M. Zurk, Source motion compensation using waveguide invariant theory, *J. Acoust. Soc. Amer.* **110**(5) (2001) 2717–2720.
4. A. M. Thode, Source ranging with minimal environmental information using a virtual receiver and waveguide invariant theory, *J. Acoust. Soc. Amer.* **108**(4) (2000) 1582–1594.
5. G. Q. Guo, Y. X. Yang, C. Sun and B. Li, Waveguide invariance structure for low frequency monostatic bottom reverberation mitigation in shallow water (in Chinese), *Acta Acustica* **34**(6) (2009) 506–514.
6. R. H. Zhang, X. X. Su and F. H. Li, Improvement of low-frequency acoustic spatial correlation by frequency-shift compensation, *Chin. Phys. Lett.* **23**(7) (2006) 1838–1841.
7. D. Z. Gao, N. Wang and H. Z. Wang, A dedispersion transform for sound propagation in shallow-water waveguide, *J. Comput. Acoust.* **18**(3) (2010) 245–257.
8. J. Bonnel, G. Le Touzé, B. Nicolas and J. Mars, Physics-based time-frequency representations for underwater acoustics: Power class utilization with waveguide-invariant approximation, *IEEE Signal Processing Magazine* **30**(6) (2013) 120–129.
9. R. Baraniuk and D. Jones, Unitary equivalence: A new twist on signal processing, *IEEE Trans. Signal Processing* **43**(10) (1995) 2269–2282.
10. J. Bonnel, B. Nicolas, J. I. Mars and S. C. Walker, Estimation of modal group velocities with a single receiver for geoacoustic inversion in shallow water, *J. Acoust. Soc. Am.* **128**(2) (2010) 719–727.
11. M. Lopatka, G. Le Touzé, B. Nicolas, X. Cristol, J. Mars and D. Fattaccioli, Underwater broadband source localization based on modal filtering and features extraction, *EURASIP Journal on Advances in Signal Processing* **2010** (2010) 1–19.

12. J. Bonnel and A. Thode, Using warping processing to range bowhead whale sounds from a single receiver, in *Proc. of the 21st International Conference of Acoustics* (*Montreal*) **19** (2013) 070066.
13. J. Bonnel, C. Gervaise, B. Nicolas and J. Mars, Single-receiver geoacoustic inversion using modal reversal, *J. Acoust. Soc. Amer.* **131** (2012) 119–128.
14. H. Q. Niu, R. H. Zhang, Z. L. Li, Y. G. Guo and L. He, Bubble pulse cancelation in the time-frequency domain using warping operators, *Chin. Phys. Lett.* **30** (2013) 084301.
15. S. H. Zhou, H. Q. Niu, Y. Ren and L. He, Fluctuating modal interference characteristics in shallow water with a seasonal thermocline, *AIP Conf. Proc.* **1495** (2012) 321–328.
16. G. Le Touzé, B. Nicolas, J. Mars and J. Lacoume, Matched representations and filters for guided waves, *IEEE Trans. Signal Process.* **57**(5) (2009) 1783–1795.
17. H. Q. Niu, R. H. Zhang and Z. L. Li, A modified warping operator based on BDRM theory in homogeneous shallow water, *SCIENCE CHINA Physics, Mechanics & Astronomy* **57**(3) (2014) 424–432.
18. H. Q. Niu, R. H. Zhang and Z. L. Li, Theoretical analysis of warping operators for non-ideal shallow water waveguides, *J. Acoust. Soc. Amer.* **136**(1) (2014) 53–65.
19. S. H. Zhou, Y. B. Qi and Y. Ren, Frequency invariability of acoustic field and passive source range estimation in shallow water, *SCIENCE CHINA Physics*, *Mechanics & Astronomy* **57**(2) (2014) 225–232.
20. Y. B. Qi, S. H. Zhou, Y. Ren, J. J. Liu, D. J. Wang and X. Q. Feng, Passive source range estimation with a single receiver in shallow water (in Chinese), *Acta Acustica* (2014) (accepted).
21. Y. B. Qi, S. H. Zhou, R. H. Zhang, B. Zhang and Y. Ren, Modal characteristic frequency in a range-dependent shallow-water waveguide and its application to source range estimation (in Chinese), *Acta Phys. Sin.* **63** (2014) 044303.
22. F. B. Jensen, W. A. Kuperman, M. B. Porter and H. Schmidt, *Computational Ocean Acoustics* (AIP Press, New York, 2000), Chap. 5.
23. G. Grachev, Theory of acoustic field invariants in layered waveguides, *Acoustical Physics* **39**(1) (1993) 33–35.
24. G. L. D'Spain and W. A. Kuperman, Application of waveguide invariants to analysis of spectrograms from shallow water environments that vary in range and azimuth, *J. Acoust. Soc. Amer.* **106**(5) (1999) 2454–2468.
25. D. Rouseff and R. C Spindel, Modeling the waveguide invariant as a distribution, *AIP Conf. Proc.* **621**(1) (2002) 137–150.
26. C. M. Bender and S. A. Orszag, *Advanced Mathematical Methods for Scientists and Engineers* (McGraw-Hill, New York, 1978), pp. 276–280.
27. M. B. Porter, The KRAKEN normal mode program, *SACLANTCEN Memorandum* (1991), SM-245.